

REPORT DOCUMENTATION PAGE			Form Approved OMB NO. 0704-0188		
<p>The public reporting burden for this collection of information is estimated to average 1 hour per response, including the time for reviewing instructions, searching existing data sources, gathering and maintaining the data needed, and completing and reviewing the collection of information. Send comments regarding this burden estimate or any other aspect of this collection of information, including suggestions for reducing this burden, to Washington Headquarters Services, Directorate for Information Operations and Reports, 1215 Jefferson Davis Highway, Suite 1204, Arlington VA, 22202-4302. Respondents should be aware that notwithstanding any other provision of law, no person shall be subject to any penalty for failing to comply with a collection of information if it does not display a currently valid OMB control number. PLEASE DO NOT RETURN YOUR FORM TO THE ABOVE ADDRESS.</p>					
1. REPORT DATE (DD-MM-YYYY) 28-08-2018		2. REPORT TYPE Article		3. DATES COVERED (From - To) -	
4. TITLE AND SUBTITLE Periodic Variation of Mutation Rates in Bacterial Genomes Associated with Replication Timing			5a. CONTRACT NUMBER W911NF-10-1-0444		
			5b. GRANT NUMBER		
			5c. PROGRAM ELEMENT NUMBER 611103		
6. AUTHORS Marcus M. Dillon, Way Sung, Michael Lynch, Vaughn S. Cooper, Michael T. Laub			5d. PROJECT NUMBER		
			5e. TASK NUMBER		
			5f. WORK UNIT NUMBER		
7. PERFORMING ORGANIZATION NAMES AND ADDRESSES Indiana University at Bloomington 509 East 3rd ST  Bloomington, IN 47401 -3654			8. PERFORMING ORGANIZATION REPORT NUMBER		
9. SPONSORING/MONITORING AGENCY NAME(S) AND ADDRESS (ES) U.S. Army Research Office P.O. Box 12211 Research Triangle Park, NC 27709-2211			10. SPONSOR/MONITOR'S ACRONYM(S) ARO		
			11. SPONSOR/MONITOR'S REPORT NUMBER(S) 58126-LS-MUR.52		
12. DISTRIBUTION AVAILABILITY STATEMENT Approved for public release; distribution is unlimited.					
13. SUPPLEMENTARY NOTES The views, opinions and/or findings contained in this report are those of the author(s) and should not be construed as an official Department of the Army position, policy or decision, unless so designated by other documentation.					
14. ABSTRACT The causes and consequences of spatiotemporal variation in mutation rates remains to be explored in nearly all organisms. Here we examine relationships between local mutation rates and replication timing in three bacterial species whose genomes have multiple chromosomes: <i>Vibrio fischeri</i> , <i>Vibrio cholerae</i> , and <i>Burkholderia cenocepacia</i> . Following five evolution experiments with these bacteria conducted in the near-absence of natural selection, the genomes of clones from each lineage were sequenced and					
15. SUBJECT TERMS Mutation rate, genome organization, periodicity, <i>Vibrio cholerae</i> , <i>Vibrio fischeri</i>					
16. SECURITY CLASSIFICATION OF:		17. LIMITATION OF ABSTRACT		15. NUMBER OF PAGES	19a. NAME OF RESPONSIBLE PERSON
a. REPORT UU	b. ABSTRACT UU	c. THIS PAGE UU	UU		Patricia Foster
				19b. TELEPHONE NUMBER 812-855-4084	

---

**REPORT DOCUMENTATION PAGE (SF298)**  
**(Continuation Sheet)**

---

**Continuation for Block 13**

Proposal/Report Number: 58126.52-LS-MUR

Report Title: Periodic Variation of Mutation Rates in Bacterial Genomes Associated with Replication Timing

Report Type: Article

**Publication Type:** Journal Article                      Peer Reviewed: Y                      **Publication Status:** 1-Published

**Journal:** mBio

Publication Identifier Type: DOI

Publication Identifier: 10.1128/mBio.01371-18

Volume: 9

Issue: 4

First Page #:

Date Submitted: 8/28/18 12:00AM

Date Published: 8/1/18 7:00AM

Publication Location:

**Article Title:** Periodic Variation of Mutation Rates in Bacterial Genomes Associated with Replication Timing

**Authors:** Marcus M. Dillon, Way Sung, Michael Lynch, Vaughn S. Cooper, Michael T. Laub

**Keywords:** Mutation rate, genome organization, periodicity, *Vibrio cholerae*, *Vibrio fischeri*

**Abstract:** The causes and consequences of spatiotemporal variation in mutation rates remains to be explored in nearly all organisms. Here we examine relationships between local mutation rates and replication timing in three bacterial species whose genomes have multiple chromosomes: *Vibrio fischeri*, *Vibrio cholerae*, and *Burkholderia cenocepacia*. Following five evolution experiments with these bacteria conducted in the near-absence of natural selection, the genomes of clones from each lineage were sequenced and analyzed to identify variation in mutation rates and spectra. In lineages lacking mismatch repair, base-substitution mutation rates vary in a mirrored wave-like pattern on opposing replichores of the large chromosome of *V. fischeri* and *V. cholerae*, where concurrently replicated regions experience similar base-substitution mutation rates. The base-substitution mutation rates on the small chromosome are less variable in both species but occur at similar rates as the concurrently replicated...

**Distribution Statement:** 1

Acknowledged Federal Support: Y

1 **Periodic variation of mutation rates in bacterial genomes associated with**  
2 **replication timing**

3  
4 Marcus M. Dillon<sup>a,b</sup>, Way Sung<sup>c,d</sup>, Michael Lynch<sup>d</sup>, and Vaughn S. Cooper<sup>b,e,f#</sup>

5  
6  
7  
8 <sup>a</sup>Department of Cell and Systems Biology, University of Toronto, Toronto, ON, CAN

9  
10 <sup>b</sup>Graduate Program in Microbiology, University of New Hampshire, Durham, NH, USA

11  
12 <sup>c</sup>Department of Bioinformatics and Genomics, University of North Carolina Charlotte,  
13 Charlotte, NC, USA

14  
15 <sup>d</sup>Department of Biology, Indiana University, Bloomington, IN, USA

16  
17 <sup>e</sup>Department of Microbiology and Molecular Genetics, University of Pittsburgh School of  
18 Medicine, Pittsburgh, PA, USA

19  
20 <sup>f</sup>Center for Evolutionary Biology and Medicine, University of Pittsburgh School of  
21 Medicine

22  
23  
24 **Corresponding Author:**

25 Vaughn Cooper  
26 425 Bridgeside Point II, 450 Technology Drive  
27 Pittsburgh, PA 15219  
28 Phone: (412)-624-1265  
29 Email: [vaughn.cooper@pitt.edu](mailto:vaughn.cooper@pitt.edu)

30  
31  
32  
33 Running title: Periodic variation in bacterial mutation rates

34  
35  
36  
37 Keywords: Mutation rate, genome organization, periodicity, *Vibrio cholerae*, *Vibrio*  
38 *fischeri*

39  
40  
41  
42 Abstract Word Count: 215

43  
44 Importance Word Count: 140

45  
46 Main Text Word Count: 5552

47 **ABSTRACT**

48 The causes and consequences of spatiotemporal variation in mutation rates remains to  
49 be explored in nearly all organisms. Here we examine relationships between local  
50 mutation rates and replication timing in three bacterial species whose genomes have  
51 multiple chromosomes: *Vibrio fischeri*, *Vibrio cholerae*, and *Burkholderia cenocepacia*.  
52 Following five evolution experiments with these bacteria conducted in the near-absence  
53 of natural selection, the genomes of clones from each lineage were sequenced and  
54 analyzed to identify variation in mutation rates and spectra. In lineages lacking  
55 mismatch repair, base-substitution mutation rates vary in a mirrored wave-like pattern  
56 on opposing replichores of the large chromosome of *V. fischeri* and *V. cholerae*, where  
57 concurrently replicated regions experience similar base-substitution mutation rates. The  
58 base-substitution mutation rates on the small chromosome are less variable in both  
59 species but occur at similar rates as the concurrently replicated regions of the large  
60 chromosome. Neither nucleotide composition nor frequency of nucleotide motifs differed  
61 among regions experiencing high and low base-substitution rates, which along with the  
62 inferred ~800 Kb wave period suggests that the source of the periodicity is not  
63 sequence-specific but rather a systematic process related to the cell cycle. These  
64 results support the notion that base-substitution mutation rates are likely to vary  
65 systematically across many bacterial genomes, which exposes certain genes to  
66 elevated deleterious mutational load.

67

68 **IMPORTANCE**

69 That mutation rates vary within bacteria genomes is well known, but the detailed study  
70 of these biases has been made possible only recently with contemporary sequencing  
71 methods. We applied these methods to understand how bacterial genomes with multiple  
72 chromosomes, like *Vibrio* and *Burkholderia*, might experience heterogeneous mutation  
73 rates because of their unusual replication and the greater genetic diversity found on  
74 smaller chromosomes. This study captured thousands of mutations and revealed wave-  
75 like rate variation that is synchronized with replication timing and not explained by  
76 nucleotide content. The scale of this rate variation over hundreds of kilobases of DNA  
77 strongly suggests that a temporally regulated cellular process may generate wave-like  
78 variation in mutation risk. These findings add to our understanding of how mutation risk  
79 is distributed across bacterial and likely also eukaryotic genomes, owing to their highly  
80 conserved replication and repair machinery.

## 81 INTRODUCTION

82 Mutation rates may vary within genomes for a variety of reasons, from straightforward  
83 causes like repetitive sequences causing polymerase slippage or the deamination and  
84 errant repair of methylated bases, to more complex causes like transcription-translation  
85 conflicts (1, 2). These processes tend to produce mutation rate heterogeneity over  
86 intervals less than 1 Kb. What is underappreciated is the potential for mutation rates to  
87 vary over longer ranges that may exceed 100 Kb and affect hundreds of genes. The  
88 prevalence and causes of long-range variation are unclear but have been attributed to  
89 effects of error prone polymerases (3), error prone repair pathways (4), and inconsistent  
90 nucleotide pools (5). If this long-range variation is common and systematic, the affected  
91 genes would be subject to greater mutational load and this process could select for  
92 gene reordering to avoid mutation risk.

93

94 On the other hand, replication timing, or the relative distance from the origin of  
95 replication, is one of the most conserved properties of orthologous genes, (6). Selection  
96 to maintain gene order has been attributed mostly to gene expression, where intragenic  
97 variation in the binding of nucleotide associated proteins (NAPs) and compaction of the  
98 nucleoid induce selection on gene order and location for optimal expression (6–9).  
99 Consequently, genes may face conflicts between the demand for optimal expression  
100 and their mutation risk, which has broad implications for genome evolution and genetic  
101 diseases. A series of comparative studies in multicellular eukaryotes (10–13), unicellular  
102 eukaryotes (12, 14), archaea (15), and bacteria (16, 17) have shown that synonymous  
103 substitution rates -- a product of all population genetic forces including mutation,

104 genetic drift, and selection -- vary across the genome and generally increase in late  
105 replicating regions. This correlation could result from higher base-substitution mutation  
106 (bpsm) rates or weaker purifying selection in late replicating regions (1, 16, 18). A  
107 powerful approach to disentangle these processes is the mutation-accumulation (MA)  
108 experiment analyzed by whole-genome sequencing (WGS), in which many replicate  
109 lineages are passaged through hundreds of single cell bottlenecks in the near absence  
110 of natural selection and all mutations are identified. Our aim was to directly test whether  
111 *de novo* mutation rates vary among genome regions, and specifically whether such  
112 long-range systematic mutation rate variation operates in bacteria.

113

114 This study builds upon several prior MA-WGS studies in diverse bacterial species.  
115 Above all, mutation rates in bacteria are remarkably low, even dropping below  $10^{-3}$   
116 <sup>3</sup>/genome/generation (1, 19). Such low rates mean that MA experiments using wild-type  
117 strains with intact mismatch repair (MMR) fail to capture enough mutations to detect  
118 long-range mutation rate variation (19–21). MA studies with MMR-deficient organisms  
119 generate much larger collections of mutations but have shown no simple, linear  
120 correlation between bpsm rates and replication timing (19, 22–25). Thus, the more rapid  
121 evolution of late-replicated genes likely results from weaker purifying selection, not  
122 increased mutation rates. More intriguingly, MA studies of MMR-deficient bacteria,  
123 including *Escherichia coli*, *Pseudomonas fluorescens*, *Pseudomonas aeruginosa*, and  
124 *Bacillus subtilis* have revealed significant non-linear or periodic variation in mutation  
125 rates among genome regions (19, 22–25).

126

127 We chose to study three bacterial species with genomes containing multiple circular  
128 chromosomes: *Vibrio cholerae*, *Vibrio fischeri*, and *Burkholderia cenocepacia* (19, 21).  
129 This is an underappreciated but not uncommon bacterial genome architecture (16, 26–  
130 28) and enables effects of chromosome location and replication timing to be  
131 distinguished. Setting aside the distinction between chromosomes and megaplasmids  
132 (29), the *Vibrio cholerae* and *Vibrio fischeri* genomes are composed of two  
133 chromosomes, while the *Burkholderia cenocepacia* genome is composed of three. In  
134 each species, the first chromosome (chr1) is largest, harbors the most essential genes,  
135 and is expressed at the highest levels (16, 30). Secondary chromosomes (chr2, chr3)  
136 also initiate replication from a single origin and are replicated bi-directionally on two  
137 replichores (28, 31, 32). While they are replicated at the same rate as the first  
138 chromosome, their origins of replication (*oriCII*) have distinct initiation requirements from  
139 those of chr1 origins (*oriCI*) (26, 33). Importantly, chr2 (or chr3) replication is delayed  
140 relative to chr1 to ensure that replication of all chromosomes terminates synchronously  
141 (28, 32, 34). Consequently, the genome region near the origin of chr1 is always  
142 replicated prior to secondary chromosomes, while late replicated regions of chr1 are  
143 replicated concurrently with chr2.

144

145 This replication timing program in bacteria with multiple circular chromosomes enabled  
146 a test of whether secondary chromosomes experience similar mutation rates and  
147 regional variation to concurrently late replicated regions of primary chromosomes. Here  
148 we report detailed analyses of the genome-wide distribution of spontaneous bpsms  
149 generated by MA-WGS experiments with MMR-deficient strains of *V. fischeri* (4313

150 bpsms) and *V. cholerae* (1022 bpsms), and spontaneous bpsms generated by MA-  
151 WGS experiments with MMR-proficient strains of *V. fischeri* (219 bpsms), *V. cholerae*  
152 (138 bpsms), and *B. cenocepacia* (245 bpsms) (19, 21). We define the patterns of  
153 fluctuations in mutation rates within each genome and assess whether this variance  
154 affects coordinately replicated regions within and among chromosomes. In the MMR-  
155 deficient lines, we find evidence of systematic variation in mutation rate that implies that  
156 the causative factors act not just spatially but also temporally with the cell cycle, a  
157 phenomenon that could apply to a broad range of organisms.

158

## 159 **RESULTS**

160 Two MMR-deficient (mutator) and three MMR-proficient (wild-type) MA-WGS  
161 experiments were founded by five different ancestral strains: a) *V. fischeri* ES114  
162  $\Delta mutS$  (*Vf*-mut), b) *V. cholerae* 2740-80  $\Delta mutS$  (*Vc*-mut), c) *V. fischeri* ES114 wild-type  
163 (*Vf*-wt), d) *V. cholerae* 2740-80 wild-type (*Vc*-wt), and e) *B. cenocepacia* HI2424 wild-  
164 type (*Bc*-wt). Forty-eight independent MA lineages were propagated for 43 days in the  
165 two mutator experiments and seventy-five MA lineages were propagated for 217 days in  
166 the three wild-type experiments. In total, successful WGS was completed on evolved  
167 clones of 19 *Vf*-mut lineages, 22 *Vc*-mut lineages, 48 *Vf*-wt lineages, 49 *Vc*-wt lineages,  
168 and 47 *Bc*-wt lineages. Despite the fact that the mutator experiments were shorter and  
169 involved fewer lineages, the vast majority of bpsms were generated in the *Vf*-mut and  
170 *Vc*-mut lineages, as their bpsm rates are 317-fold and 85-fold greater than those of their  
171 wild-type counterparts, respectively. Consequently, effects of genomic position on bpsm  
172 rates can be studied in much greater detail in the mutator lineages, where adequate

173 numbers of bpsms are distributed across the genome at intervals as short as 10 Kb  
174 (Table 1), the approximate length of bacterial microdomains (7).

175  
176 In comparing the overall bpsm rates between chromosomes in the mutator lineages, we  
177 observed that the bpsm rate on chr1 and chr2 of *V. fischeri* were not statistically  
178 distinguishable ( $\chi^2 = 0.11$ , df = 1, p = 0.741), while the bpsm rate on chr1 of *V. cholerae*  
179 was slightly higher than the rate of chr2 ( $\chi^2 = 4.54$ , df = 1, p = 0.0331) (19). However,  
180 even in *V. cholerae*, the variation in bpsm rates was minimal between chromosomes  
181 and our data suggested that considerably greater variation may exist within  
182 chromosomes (19). To determine the effects of genomic position on bpsm rates on a  
183 finer scale, we analyzed bpsm rates among intervals of varying size (10-500Kb)  
184 extending bi-directionally from the *oriCI* as the replication forks proceed during  
185 replication. Rates on chr2 were analyzed using the same intervals as chr1 but according  
186 to the inferred replication timing of *oriCI* (Figure S1A). This enables direct comparisons  
187 between concurrently replicated intervals on both chromosomes. To illustrate how this  
188 analysis works, we plotted the patterns of bpsm rates from a recent *E. coli* mutator MA  
189 experiment where mutation rates were demonstrated to vary in a wave-like pattern that  
190 is mirrored on the two replichores of its singular circular chromosome (20, 22) (Figure  
191 S1B). If replication timing is responsible for this pattern, a hypothetical secondary  
192 chromosome in *E. coli* would be expected to mirror concurrently replicated (late  
193 replicating) regions on the primary chromosome (Figure S1B).

194

195 **Base-substitution mutation rates are wave-like on chr1 in mutator lines.** Mutation  
196 rates were not uniformly distributed across 10-500Kb intervals on chr1 in either the *Vf*-  
197 mut or the *Vc*-mut MA experiments (Supplementary Data), but we could not reject the  
198 null hypothesis of uniform rates on chr2, which has lower variance in bpsm rates.  
199 Variation in bpsm rates on chr1 in both *Vf*-mut and *Vc*-mut experiments follows a wave-  
200 like pattern that is mirrored on both replichores bi-directionally from the origin of  
201 replication (Figure 1A, B). This mirrored pattern is evident at multiple interval sizes and  
202 is consistent with what has been reported on the single chromosome of *E. coli* (22),  
203 although the length of the wave periods observed here are shorter (Figure S1B). The  
204 waveform of bpsm rates is low near *oriCI*, increases to its peak approximately 600 Kb  
205 from the *oriCI* on both replichores, and declines into another valley before rising and  
206 falling again in the approach to the replication terminus. Two distinct waves can be seen  
207 on each replichore of chr1 (Figure 1A, B) but are less evident on chr2 (Figure S2). We  
208 focused our most detailed analyses of patterns of bpsm rate variation at the 100 Kb  
209 interval because it maximizes bpsms/interval while retaining two apparently mirrored  
210 bpsm rate waves on each replichore. Over 100Kb intervals, we see a significantly  
211 positive correlation between bpsm rates of concurrently replicated regions on the left  
212 and right replichores of chr1 in both *V. fischeri* and *V. cholerae* (Figure 2A, B). This  
213 relationship is also significant at most other interval lengths (Supplementary Data), but  
214 we find no such relationship when comparing 100 Kb intervals on the left and right  
215 replichores of chr2 as a consequence of its lower variance in bpsm rate.  
216

217 **Concurrently replicated regions between chromosomes exhibit similar mutation**  
218 **rates.** Given the observed relationship between bpsm rates of concurrently replicated  
219 regions on chr1, we might also expect late replicated regions of chr1 to experience  
220 similar bpsm rates as chr2 because of their concurrent replication. To study this  
221 relationship, we mapped the patterns of bpsm rates in 100 Kb intervals on chr2 to those  
222 of late replicated 100 Kb intervals on chr1 for both *Vf*-mut and *Vc*-mut (Figure S1).  
223 Fluctuations in bpsm rates on chr2 resemble those of late replicated regions on chr1 in  
224 both species (Figure 3A, B), but linear correlations in bpsm rates between chr1 and chr  
225 2 were not significant (Supplementary Data). However, this lack of significant  
226 relationship may be a reflection of late replicated regions generally experiencing lower  
227 variance in bpsm rates than chr1 as a whole and given the strong resemblance in bpsm  
228 rate fluctuations between chr2 and concurrently late replicated regions of chr1, we  
229 attempted to falsify this match by correlating chr2 bpsm rates by correlating chr2 bpsm  
230 rates with all possible interval combinations on the right and left replichores of chr1. For  
231 *Vf*-mut, the lowest sum of the residuals ( $14.01 \times 10^{-8}$ ) occurs when the chr2 intervals  
232 were mapped to the concurrently late replicated intervals on chr1 (Figure 3A;  
233 Supplementary Data). This same pattern was found for *Vc*-mut (Figure 3B;  
234 Supplementary Data). Thus, despite no significant linear correlation in mutation rate  
235 periodicity between chr1 and chr2, the spatial variation in bpsm rates on chr2 most  
236 closely resembles the rates of concurrently replicated regions on chr1 in both *V.*  
237 *cholerae* and *V. fischeri*. Interestingly, the delayed replication and small size of chr2  
238 allows it to narrowly avoid the peak bpsm rates on the right and left replichores of chr1

239 in both *Vf*-mut and *Vc*-mut (Figure 3A, B). Thus, genes on chr2 may be subjected to  
240 less deleterious load than many of the genes on chr1, particularly in *V. cholerae*.

241  
242 **Wavelet transformations capture periodicities in base-substitution mutation rates.**

243 Recognizing that regional or cyclic variation in mutation rates may not be captured by  
244 linear models, we used wavelet transformations to characterize periodicities in the  
245 mirrored wave-like patterns in bpsm rates observed in this study. Bpsm rates on each  
246 chromosome in the *Vf*-mut and *Vc*-mut studies were transformed using the Morlet  
247 wavelet (35), which can reveal time-associated changes in the frequency of bpsms and  
248 has been successfully used in ecological time series analyses (36). This method was  
249 used to identify significant wave periods in bpsm rates on chr1 and chr2 and any  
250 variation in period length or amplitude across the chromosome. Significant wave periods  
251 of approximately 1.6 Mb and 0.8 Mb extend clockwise from *oriCI* in the *Vf*-mut lineages  
252 (Figure 4A). The single, long-period wave of 1.6 Mb is well supported across each  
253 replicore, while the shorter ~0.8 Mb period wave is significant across most of chr1 but  
254 its inferred length varies between 0.6 and 1.0 Mb. Thus, there are two synchronous  
255 periods per replicore or four periods in total around the chromosome, which are also  
256 clearly evident in Figure 1. These same two wave periods of approximately 1.6 Mb and  
257 0.8 Mb were also observed in the bpsm rate data found on chr1 in the *Vc*-mut lineages  
258 (Figure 5E).

259  
260 Using only these wave models, we successfully reproduced the apparent periodicity of  
261 the 100 Kb data in both the *Vf*-mut and *Vc*-mut lineages (Figure 4B, F). Next, using the

262 cross-wavelet transformation method to identify shared periodicities between  
263 replichores (35), we found that the wave model derived from one replichore predicts the  
264 behavior of the other (Figure S3A, B). It is also noteworthy that the statistically  
265 synchronous waves become smaller near the replication terminus, particularly in the *Vf*-  
266 *mut* lineages (Figure S3A, B), which is also apparent in the raw data presented in  
267 Figure 1. Perhaps because of this lower variation in late replicated regions, these  
268 modeling efforts were not successful on chr2 for either the *Vf*-mut or the *Vc*-mut  
269 experiment (Figure 4C, D, G, H).

270

271 **Replication-associated periodicity results from specific forms of base-**  
272 **substitution mutations.** Nucleotide content varies across chromosomes and could  
273 conceivably underlie variation in bpsm rates among 100 Kb intervals. To address this  
274 possibility, we focused on A:T>G:C and G:C>A:T transitions in the *Vf*-mut and *Vc*-mut  
275 studies, as these two forms of bpsm represent 97.93% and 98.34% of all observed  
276 bpsms, respectively (19). Nucleotide composition did not vary significantly among 100  
277 Kb intervals on chr1 or chr2. However, the spectra of bpsms corrected for nucleotide  
278 content varied significantly among intervals on chr1 in both the *Vf*-mut and *Vc*-mut MA  
279 experiments (Chi-square test; A:T>G:C: *Vf*-mut -  $\chi^2 = 62.26$ ,  $df = 29$ ,  $p = 0.0003$ , *Vc*-mut  
280 -  $\chi^2 = 49.04$ ,  $df = 29$ ,  $p = 0.0110$ ; G:C>A:T: *Vf*-mut -  $\chi^2 = 120.69$ ,  $df = 29$ ,  $p < 0.0001$ ,  
281 *Vc*-mut -  $\chi^2 = 111.19$ ,  $df = 29$ ,  $p < 0.0001$ ). On chr2, only G:C>A:T substitutions in the  
282 *Vf*-mut study varied among intervals ( $\chi^2 = 26.81$ ,  $df = 15$ ,  $p = 0.0300$ ). Interestingly,  
283 G:C>A:T mutation rates exhibit the greatest variation among chr1 intervals in both the  
284 *Vf*-mut and *Vc*-mut studies, and the positive correlations in bpsm rates on opposing

285 replichores are driven largely by G:C>A:T, not A:T>G:C bpsms (Figure S4). The  
286 periodicity in bpsm rates in the *Vf-mut* and *Vc-mut* lines is therefore not caused by  
287 differences in nucleotide content but is predominantly caused by G:C>A:T transitions.

288  
289 The immediate 5' and 3' nucleotide context of the mutated base can also influence rates  
290 and could conceivably lead to periodicity if trimers vary among intervals. Indeed,  
291 genome-wide bpsm rates in both the *Vf-mut* and *Vc-mut* studies vary more than 50-fold  
292 depending on the 5' and 3' bases flanking the site of the bpsm (Figure S5). This  
293 phenomenon has been found in several bacterial genomes and was found to be driven  
294 by sites neighboring G:C base pairs or dimers including alternating pyrimidine–purine  
295 and purine–pyrimidine nucleotides having significantly elevated mutation rates (24).  
296 However, the product of trimer abundance and specific mutation rates cannot explain  
297 the distribution of bpsms measured here on chr1 in either *V. cholerae* and *V. fischeri*  
298 (Figure S5).

299  
300 **Low base-substitution mutation rates in wild-type lineages reveal modest**  
301 **regional variation.** Despite conducting longer MA experiments (217 days vs 43 days)  
302 and sequencing more lineages (48 vs 22) derived from wild-type, MMR+ ancestors of *V.*  
303 *fischeri*, *V. cholerae*, and *B. cenocepacia*, considerably fewer bpsms accumulated in  
304 these lines than MMR- lines. Consequently, we cannot reject the null hypothesis that  
305 bpsms are uniformly distributed across chr1, chr2, and chr3 (for *Bc*) in the *Vf*-wt, *Vc*-wt,  
306 or *Bc*-wt MA experiments (Supplementary Data). Furthermore, coordinately replicated  
307 regions of chr1 and chr2 also did not exhibit correlated mutation rates, likely because of

308 low sample sizes (Figure 5A, B, C). Only a mean of 4.65 (0.38), 3.29 (0.28), and 3.08  
309 (0.22) (SEM) bpsms per 100 Kb interval were detected for the *Vf*-wt, *Vc*-wt, and *Bc*-wt  
310 MA lineages, respectively. Using effect size estimates derived from the significant  
311 patterns in MMR- lines (see Supplemental Methods), we estimate that the 132  
312 mutations found on chr1 in the *Vf*-wt experiment would reveal a significantly non-  
313 uniform distribution of bpsms in only 19.46% of cases. The same analysis applied to the  
314 *Vc*-wt experiment predicts that significant regional variation in bpsms would be identified  
315 only 43.95% of the time. Further, applying effects from the *Vc*-mut to the *Bc*-wt  
316 experiment suggests that significant regional variation would be seen on chr1 in 55.16%  
317 of cases. Greater replication may be needed to capture more mutations in wild-type  
318 genomes to determine whether the periodicity in mutation rates seen in mutator lines  
319 also occurs in wild-type genomes, but we did observe that the patterns of bpsm rate  
320 variation in the *Vc*-wt experiment, where the effect size was largest, correlate with that  
321 of the corresponding mutator experiment, which implies a common underlying process  
322 for variation in mutator and wild-type bpsm rates (linear regression, 100 Kb intervals;  
323 *Vc*-wt – *Vc*-mut:  $F = 5.07$ ,  $df = 38$ ,  $p = 0.0303$ ,  $r^2 = 0.12$ ).

324

## 325 **DISCUSSION**

326 Variation in mutation rates among genome regions can have important implications for  
327 genome evolution and diseases, including most cancers (6–8, 37–40). One of the most  
328 conserved properties of genome organization is the relative distance of genes from the  
329 origin of replication (6, 41), which is expected to result in the long-term conservation of  
330 traits like expression and mutation rates for genes harbored in divergent genomes.

331 Consequently, molecular modifications that change genome-wide patterns of replication  
332 timing, expression, and mutation rates could increase the probability of acquiring  
333 defective alleles in typically conserved regions, leading to disease. Indeed, alteration of  
334 the replication timing program can be an early step in carcinogenesis and a number of  
335 other somatic disease states (37). However, given the remarkable diversity in genome  
336 architecture across the tree of life, we still have much to learn about the nature of  
337 regional patterns of variation in bpsm rates and the genomic features and molecular  
338 processes that govern them.

339  
340 Periodic variation in bpsm rates that is mirrored on the two replichores of bacterial  
341 chromosomes has been observed in genomes of some single-chromosome bacteria  
342 that are MMR-deficient (22, 25), yet not all species appear to experience this periodicity  
343 (23), and the underlying causes of periodic variation in bacterial bpsm rates are  
344 unknown. Here we demonstrate that MMR-deficient bacterial genomes with multiple  
345 chromosomes display mirrored, wave-like patterns of bpsm rates on chr1 (Figure 1A,  
346 B), and although we cannot reject the null hypothesis that bpsm rates are uniform on  
347 chr2, the patterns of bpsm rates on chr2 best match those of concurrently replicating  
348 regions on chr1 (Figure 3A, B). Furthermore, much of the genome-wide variation in  
349 bpsm rates that we observe appears to be generated by G:C>A:T transitions in both the  
350 *Vf*-mut and *Vc*-mut studies. Three MA experiments with MMR-proficient genomes hint at  
351 regional variation in bpsm rates, but these studies were insufficiently powered to reject  
352 the null hypothesis of uniformity. Nonetheless, shared periodicities in mutation rates  
353 between replichores and coarse similarities across chromosome regions that are

354 coordinately replicated suggests strongly that mutation rates are affected by one or  
355 more common, global processes. Such a process influences replication fidelity  
356 throughout the genome at different active replication forks and causes bpsm rates to  
357 occur at a minimum level near the replication origin, rise to roughly 2-4 times these  
358 rates, then decline and repeat this cycle before replication termination. If physically  
359 separate genome regions share common mutation rates because of their shared  
360 replication timing, their genetic content may also be subject to common evolutionary  
361 forces.

362  
363 This study cannot directly test the potential causes of mutation rate variation, but the  
364 bpsm patterns are more consistent with certain causes. First, nucleotide context can  
365 generate heterogeneous bpsm rates because certain nucleotides or nucleotide contexts  
366 are more prone to incur bpsms than others (20, 23, 24, 42, 43), and there is reason to  
367 believe that concurrently replicated regions on opposing replichores contain  
368 symmetrical gene content (41). Although we find that bpsm rates in both the *Vf*-mut and  
369 *Vc*-mut studies vary more than 50-fold depending on the bases flanking the site of the  
370 bpsm (Figure S5), this variation cannot explain the overall rate periodicity.

371  
372 The replication machinery itself may also generate heterogeneous bpsm rates because  
373 of biased usage of error prone polymerases (3) or repair pathways (4) in certain  
374 genome regions. Both mechanisms have been invoked to explain why substitution rates  
375 scale positively with replication timing (4, 10–17), but the majority of these studies were  
376 performed in eukaryotes, and it is difficult to imagine how they might create the mirrored

377 wave-like patterns of bpsm rates observed in bacterial chromosomes across 100 Kb  
378 intervals. Indeed, a series of MA studies in *E. coli* have shown that error-prone  
379 polymerases have minimal effects on mutation rates in the absence of DNA damage or  
380 stress (44).

381

382

383 Other genomic features that vary systematically with replication timing like binding of  
384 nucleoid-associated proteins (NAPs), transcription levels, and compaction of the  
385 bacterial nucleoid are also candidates for explaining our observed patterns of bpsm  
386 rates (6–9, 45). Sigma factors, DNA gyrase, and a number of NAPs have mirrored  
387 patterns of activity on the right and left replichores of the single chromosome in *E. coli*  
388 (6), possibly resulting from their concurrent replication. The resultant negative DNA  
389 superhelicity does correlate positively with the mirrored wave-like patterns of bpsm rates  
390 on opposing replichores of *E. coli* (22) and patterns of extant sequence variation are  
391 significantly impacted by NAPs that bind the DNA at different growth phases (9).  
392 However, effects of NAPs on sequence variation among published genomes are  
393 relatively weak and unlikely to produce the 2-4 fold changes in bpsm rates observed  
394 across the long interval lengths used in this study (9). While transcription levels may  
395 also impact bpsm rates through gene expression and replication-transcription conflicts  
396 (46), oscillations in expression patterns and gene density are not consistent with  
397 concurrently replicated regions experiencing similar expression levels (47), and  
398 expression has not been significantly correlated with the patterns of bpsm rates in *E.*  
399 *coli* and other species (1, 22).

400  
401 The G:C>A:T and G:C>T:A bpsm that drive much of the observed periodicity are  
402 consistent with damage induced by reactive oxygen species (ROS) (Figure S4). It is  
403 conceivable that the plate growth conditions in these MA experiments generate ROS  
404 and thus more oxidized bases such as O<sup>6</sup>-methylguanine (O<sup>6</sup>-meG) and 8-oxo-guanine  
405 (8-oxo-G) (48, 49). The O<sup>6</sup>-meG modification commonly results in G:C>A:T mutations,  
406 while the 8-oxo-G modification commonly results in G:C>T:A mutations. These  
407 mutations are typically corrected by MMR and thus should be more common in MMR  
408 deficient MA lines. It remains unclear how either the origin or failed repair of ROS-  
409 induced mutations would be periodic with respect to replication timing. Conceivably,  
410 early-replicated nucleotides on Chr1 might be repaired more frequently by alternative  
411 pathways like translesion synthesis (48) and/or access to these repair complexes might  
412 be diluted with each new round of replication. This hypothesis could be tested by MA-  
413 WGS experiments under conditions that alter ROS exposure (44). For example, one  
414 recent experiment that focused on how the antibiotic norfloxacin influenced mutation  
415 rates in *E. coli* also tested effects of added peroxide because antibiotics may kill by  
416 ROS (50). Remarkably, this study also found periodic mutation rates that were mirrored  
417 on both replichores in the peroxide-treated lines, but no periodicity was seen in the  
418 norfloxacin-treated lines (potentially because of slower growth), indicating that mutation-  
419 rate periodicity may be induced by cyclical ROS-mediated effects.

420  
421 With these alternative explanations in mind, we suggest that the most straightforward  
422 dynamic that could produce wave-like bpsm rates is variation in levels of

423 deoxyribonucleotides (dNTPs). We describe a simple model of how dNTPs per  
424 replication fork may vary with *Vibrio* replication in Figure 6. Synthesis of dNTPs is  
425 controlled by levels of ribonucleotide reductase (RNR), whose production is coordinated  
426 with the rate of DNA synthesis but reaches its maximum following the onset of DNA  
427 replication to meet demand (51, 52). High levels of dNTPs are mutagenic in many  
428 organisms because of increased probability of misincorporation (52–54). In slow-  
429 growing bacteria whose division rates exceed the time required for chromosome  
430 replication, dNTP availability should increase after the start of replication and transiently  
431 increase the mutation rate but then decline to a baseline (Figure 6A, B). This predicts  
432 that slow growth should cause no mutation-rate periodicity, as the results from  
433 antibiotic-limited *E. coli* MA lines suggest (50). However, when bacterial generation  
434 times are faster than the time required for chromosome replication, which is  
435 commonplace for fast-growing species like *E. coli* or *Vibrio*, new rounds of replication  
436 are initiated and proceed before the first round concludes (55). Multi-chromosome  
437 genomes like those of *Vibrio* species require the additional firing of *oriC2*, which  
438 generates another burst of dNTP synthesis (Figure 6C, D). Consequently, fast-growing  
439 bacteria may experience multiple pulses of elevated RNR activity as origins fire (51), but  
440 the mutational effects of successive pulses of dNTP synthesis should be diluted across  
441 a growing number of active replication forks. We suggest this dynamic can simply  
442 generate the wave-like bpsm pattern observed in these experiments (Figure 1, Figure 6)  
443 as well as those previously reported in *E. coli* (22). Importantly, subsequent rounds of  
444 overlapping replication of either chromosome would only marginally affect the basic  
445 periodicity because dNTPs are diluted across multiple replication forks. Further, the

446 model may explain two key features of the waves observed in our MA experiments - the  
447 greater amplitude of the first wave nearer to the origin and the lower overall variance in  
448 mutation rates in late-replicated regions, which results from dNTP bursts being diluted  
449 across more active replication forks (Figure 3). This model may also explain why not all  
450 bacterial genomes appear to experience periodic mutation rates (23) if they grow more  
451 slowly than the time for chromosome replication. We acknowledge that this model is  
452 speculative and requires considerable additional study, although the associations  
453 between replication dynamics and RNR activity and dNTP pools and mutation rates are  
454 both well supported (53, 56–58). A related possibility is that this periodicity arises from  
455 imbalances between rNTP and dNTP pools, which has been demonstrated to be  
456 mutagenic (53, 59, 60). At a minimum, this simple model relating ribonucleotide  
457 availability with mutation-rate periodicity is empirically testable by additional MA-WGS  
458 with defined mutants and altered growth conditions.

459  
460 The conserved patterns of bpsm rates across concurrently replicated regions of MMR-  
461 lines also raises the question of whether these mutation biases influence the evolution  
462 of *Vibrio* genomes. In our previous studies of the mutation spectra from these  
463 experiments, higher rates of particular mutations were indeed found at synonymous  
464 sites among extant *Vibrio* and *Burkholderia* genomes (21, 61). If natural bpsm rates are  
465 in fact periodic in nature, we would expect genetic variation among strains to positively  
466 correlate with the bpsm rates in our defined 100 Kb intervals, particularly on chr1. We  
467 calculated the average pairwise synonymous (dS) and non-synonymous (dN)  
468 substitution rates in these intervals of *V. fischeri* and *V. cholerae* genomes (see

469 Methods) and find a significant positive correlation for dS on chr1 but not on chr2 in *V.*  
470 *fischeri* (Figure S6). As expected from stronger selection on nonsynonymous sites, no  
471 significant correlation between dN and bpsm rates was found on either chromosome  
472 (Figure S6). No significant correlations between dS or dN and bpsm rates were found  
473 on either chromosome of *V. cholerae* (Figure S6). The scant correlations between  
474 evolutionary rates in coding sequences and spontaneous mutation rates may simply  
475 reflect that selection operating on both synonymous and non-synonymous sites is quite  
476 strong in bacteria (62). Alternatively, the natural patterns of bpsm rates in *V. fischeri* and  
477 *V. cholerae* may not be consistent with those observed in MMR- lines, which are  
478 strongly biased towards transition mutations. A more extensive study of the mutation  
479 spectra of wild-type genomes both experimentally and in natural isolates will determine  
480 the extent to which mutation-rate periodicity shapes genome evolution.

481  
482 In summary, we have shown that bpsm rates in MMR-deficient lineages of *V. cholerae*  
483 *and V. fischeri* are non-uniformly distributed on chr1 and vary in a mirrored wave-like  
484 pattern that extends bi-directionally from the origin of replication. In contrast, late-  
485 replicated regions of chr1 and the entirety of chr2 experience more constant bpsm  
486 rates. These observations suggest that concurrently replicated regions of bacterial  
487 genomes experience similar bpsm rates prior to MMR, which could be governed by a  
488 number of temporally regulated cellular processes, including ROS, variation in dNTP  
489 pools, and the availability of replication machinery with secondary rounds of replication.  
490 We encourage research to disentangle effects of these cellular processes on bpsm  
491 rates (see for example (63)) as well as the signatures of these processes in natural

492 populations, which will deepen our understanding of how mutation rates vary within  
493 genomes. Recalling that the relative distance of genes from the origin of replication is  
494 highly conserved across broad phylogenetic distances for a variety of functional reasons  
495 (6), it is quite possible that some genes are exposed to elevated mutational load while  
496 others are more shielded. In light of the growing effort towards evolutionary forecasting  
497 in microbial genomes (64), the need to determine whether the probability of new  
498 mutations substantively differs between genome regions is all the more pressing.

499

## 500 **METHODS**

501 **Bacterial strains and culture conditions.** MMR-deficient ancestors were generated by  
502 replacing the *mutS* gene in *V. fischeri* ES114 and *V. cholerae* 2740-80 with an  
503 erythromycin resistance cassette, as described previously (65–68). Complete genome  
504 sequences of these ancestors are publicly available (69, 70) or were generated by us  
505 for this project (71). Replication origins were determined using Ori-finder (19, 72, 73).

506 MA experiments with *Vf*-mut and *Vf*-wt were conducted on tryptic soy agar (TSA) plates  
507 plus NaCl (30 g/liter tryptic soy broth powder, 20 g/liter NaCl, 15 g/liter agar) and  
508 incubated at 28°. MA experiments with *Vc*-mut, *Vc*-wt, and *Bc*-wt were conducted on  
509 TSA (30 g/liter tryptic soy broth powder, 15 g/liter agar) and incubated at 37°. MA  
510 experiments with MMR- lines involved 48 independent lineages founded from single  
511 colonies of *Vf*-mutS or *Vc*-mutS and were propagated daily for 43 days. MA  
512 experiments with WT lines involved 75 lineages founded from single colonies of *Vf*, *Vc*,  
513 or *Bc* and were propagated daily for 217 days (21, 61).

514

515 **Base-substitution mutation rate analysis at different genome intervals.** Genomes  
516 were divided into intervals of 10 Kb, 25 Kb, 50 Kb, 100 Kb, 250 Kb, and 500 Kb, and  
517 bpsms were categorized by interval and location. On chr1, these intervals start at *oriCI*  
518 and extend bi-directionally to the replication terminus to mimic the progression of the  
519 two replication forks. Rates of bpsm were analyzed on secondary chromosomes  
520 similarly but intervals were measured relative to the initiation of replication of *oriCI*  
521 rather than to *oriCII* (Figure S1). This enables direct comparisons between concurrently  
522 replicated intervals on chr1 and chr2 based on established models of secondary  
523 chromosome replication timing in *V. cholerae* (28, 32, 34). Matched intervals of the  
524 same length were defined on each chromosome (n.b. chromosomes are not perfectly  
525 divisible by interval lengths so some intervals are shorter). Bpsm rates in each interval  
526 were calculated as the number of mutations observed in each interval, divided by the  
527 product of the total number of sites analyzed in that interval across all lines and the total  
528 number of generations of mutation accumulation, so rates in shorter intervals could be  
529 directly compared to the full-length intervals. For independent analyses of A:T>G:C and  
530 G:C>A:T mutations, bpsm rates were calculated as the number of mutations observed  
531 in each interval, divided by the product of the total number of sites in that interval that  
532 could lead to the bpsm being analyzed (A+T sites for A:T>G:C; G+C sites for G:C>A:T)  
533 and the total number of generations of mutation accumulation.

534  
535 **Wavelet Transformations.** We used the R package WaveletComp to evaluate  
536 properties of the wave-like patterns in bpsm rates in *Vf* and *Vc* and to test whether  
537 waves on opposing replichores were synchronous (35). The periodicity of bpsm rates on

538 each chromosome of the *Vf*-mut and *Vc*-mut lineages at an interval length of 100 Kb  
539 was analyzed, treating each chromosome as a univariate series starting at the origin of  
540 replication and extending clockwise around the chromosome. WaveletComp uses the  
541 Morlet wavelet to transform the series of mutation rates then tests the null hypothesis of  
542 no periodicity for all combinations of intervals and periods (35). We performed this  
543 analysis using the “white.noise” method, with no smoothing, and a period range of 0.2  
544 Mb to the entire length of the respective chromosomes. Default settings were used for  
545 all other parameters.

546  
547 To test whether opposing replichores on Chr1 were synchronous, we used a cross-  
548 wavelet transformation (35) to test the null-hypothesis that no joint periodicity  
549 (synchronicity) exists among the two series as they traverse the primary chromosome in  
550 opposite directions. We used default settings but turned off smoothing and specified a  
551 period range of 0.2 Mb to the entire length of Chr1 in both *V. fischeri* and *V. cholerae*.

552  
553 **Sequencing and Mutation Identification.** Methods for genome sequencing, mutation  
554 identification, and evolutionary rate analyses are described in Supplementary text.

555  
556 **Data Availability.** Accession numbers for all of the whole-genome sequencing data  
557 produced by this study are PRJNA256340 for *V. fischeri*, PRJNA256339 for *V. cholerae*,  
558 and PRJNA326274 for *B. cenocepacia*.

559

560 **ACKNOWLEDGMENTS**

561 We thank Cheryl Whistler, Randi Foxall, and Brian VanDam for technical support and  
562 Kevin Culligan, Greg Lang, Jeffrey Lawrence, and Pat Foster for helpful discussion.  
563 M.D., W.S., M.L., and V.C. designed the research; M.D., and W.S. performed the  
564 research; M.D. analyzed the data; and M.D., and V.C. wrote the paper. The authors  
565 declare no conflict of interest.

566

567 This work was supported by the Multidisciplinary University Research Initiative Award  
568 from the US Army Research Office (W911NF-09-1-0444 to ML, P. Foster, H. Tang, and  
569 S. Finkel); a National Science Foundation CAREER Award (DEB-0845851 to VSC), and  
570 NASA Astrobiology Institute CAN-7 NNA15BB04A to VSC.

571 **REFERENCES**

- 572 1. Lynch M, Ackerman MS, Gout J-F, Long H, Sung W, Thomas WK, Foster PL. 2016.  
573 Genetic drift, selection and the evolution of the mutation rate. *Nat Rev Genet* 17:704–714.
- 574 2. Zhu YO, Siegal ML, Hall DW, Petrov DA. 2014. Precise estimates of mutation rate and  
575 spectrum in yeast. *Proc Natl Acad Sci U S A* 111:E2310-8.
- 576 3. Courcelle J. 2009. Shifting replication between IInd, IIIrd, and IVth gears. *Proc Natl Acad*  
577 *Sci U S A* 106:6027–6028.
- 578 4. Lang GI, Murray AW. 2011. Mutation rates across budding yeast chromosome VI are  
579 correlated with replication timing. *Genome Biol Evol* 3:799–811.
- 580 5. Zhang XL, Mathews CK. 1995. Natural DNA precursor pool asymmetry and base  
581 sequence context as determinants of replication fidelity. *J Biol Chem* 270:8401–8404.
- 582 6. Sobetzko P, Travers A, Muskhelishvili G. 2012. Gene order and chromosome dynamics  
583 coordinate spatiotemporal gene expression during the bacterial growth cycle. *Proc Natl*  
584 *Acad Sci U S A* 109:E42–E50.
- 585 7. Dorman CJ. 2013. Genome architecture and global gene regulation in bacteria: making  
586 progress towards a unified model? *Nat Rev Microbiol* 11:349–355.
- 587 8. Dame RT, Kalmykova OJ, Grainger DC. 2011. Chromosomal macrodomains and  
588 associated proteins: Implications for DNA organization and replication in gram negative  
589 bacteria. *PLoS Genet*.
- 590 9. Warnecke T, Supek F, Lehner B. 2012. Nucleoid-associated proteins affect mutation  
591 dynamics in *E. coli* in a growth phase-specific manner. *PLoS Comput Biol* 8:e1002846.

- 592 10. Chen C-L, Rappailles A, Duquenne L, Huvet M, Guilbaud G, Farinelli L, Audit B,  
593 D'Aubenton-Carafa Y, Arneodo A, Hyrien O, Thermes C. 2010. Impact of replication timing  
594 on non-CpG and CpG substitution rates in mammalian genomes. *Genome Res* 20:447–  
595 457.
- 596 11. Stamatoyannopoulos JA, Adzhubei I, Thurman RE, Kryukov G V, Mirkin SM, Sunyaev SR.  
597 2009. Human mutation rate associated with DNA replication timing. *Nat Genet* 41:393–  
598 395.
- 599 12. Herrick J. 2011. Genetic variation and DNA replication timing, or why is there late  
600 replicating DNA? *Evolution* 65:3031–3047.
- 601 13. Mugal CF, Wolf JBW, Von Grünberg HH, Ellegren H. 2010. Conservation of neutral  
602 substitution rate and substitutional asymmetries in mammalian genes. *Genome Biol Evol*  
603 2:19–28.
- 604 14. Agier N, Fischer G. 2012. The mutational profile of the yeast genome is shaped by  
605 replication. *Mol Biol Evol* 29:905–913.
- 606 15. Flynn KM, Vohr SH, Hatcher PJ, Cooper VS. 2010. Evolutionary rates and gene  
607 dispensability associate with replication timing in the archaeon *Sulfolobus islandicus*.  
608 *Genome Biol Evol* 2:859–869.
- 609 16. Cooper VS, Vohr SH, Wrocklage SC, Hatcher PJ. 2010. Why genes evolve faster on  
610 secondary chromosomes in bacteria. *Plos Comput Biol* 6:e1000732.
- 611 17. Mira A, Ochman H. 2002. Gene location and bacterial sequence divergence. *Mol Biol Evol*  
612 19:1350–1358.

- 613 18. Ochman H. 2003. Neutral mutations and neutral substitutions in bacterial genomes. *Mol*  
614 *Biol Evol* 20:2091–2096.
- 615 19. Dillon MM, Sung W, Lynch M, S. C V. 2017. Genome-wide biases in the rate and  
616 molecular spectrum of spontaneous mutations in *Vibrio cholerae* and *Vibrio fischeri*. *Mol*  
617 *Biol Evol* 34:93–109.
- 618 20. Lee H, Popodi E, Tang HX, Foster PL. 2012. Rate and molecular spectrum of spontaneous  
619 mutations in the bacterium *Escherichia coli* as determined by whole-genome sequencing.  
620 *Proc Natl Acad Sci U S A* 109:E2774–E2783.
- 621 21. Dillon MM, Sung W, Lynch M, Cooper VS. 2015. The rate and molecular spectrum of  
622 spontaneous mutations in the GC-rich multichromosome genome of *Burkholderia*  
623 *cenocepacia*. *Genetics* 200:935–946.
- 624 22. Foster PL, Hanson AJ, Lee H, Popodi EM, Tang HX. 2013. On the mutational topology of  
625 the bacterial genome. *G3-Genes Genomes Genet* 3:399–407.
- 626 23. Long H, Sung W, Miller SF, Ackerman MS, Doak TG, Lynch M. 2014. Mutation rate,  
627 spectrum, topology, and context-dependency in the DNA mismatch repair (MMR) deficient  
628 *Pseudomonas fluorescens* ATCC948. *Genome Biol Evol* 7:262–271.
- 629 24. Sung W, Ackerman MS, Gout J-F, Miller SF, Williams E, Foster PL, Lynch M. 2015.  
630 Asymmetric context-dependent mutation patterns revealed through mutation-accumulation  
631 experiments. *Mol Biol Evol* 32:1672–1683.
- 632 25. Dettman JR, Sztepanacz JL, Kassen R. 2016. The properties of spontaneous mutations in  
633 the opportunistic pathogen *Pseudomonas aeruginosa*. *BMC Genomics* 17:27–41.

- 634 26. Egan ES, Fogel MA, Waldor MK. 2005. Divided genomes: Negotiating the cell cycle in  
635 prokaryotes with multiple chromosomes. *Mol Microbiol*.
- 636 27. Ochman H. 2002. Bacterial evolution: Chromosome arithmetic and geometry. *Curr Biol*  
637 12:R427–R428.
- 638 28. Val M-E, Soler-Bistué A, Bland MJ, Mazel D. 2014. Management of multipartite genomes:  
639 the *Vibrio cholerae* model. *Curr Opin Microbiol* 22:120–126.
- 640 29. Agnoli K, Schwager S, Uehlinger S, Vergunst A, Viteri DF, Nguyen DT, Sokol PA, Carlier  
641 A, Eberl L. 2012. Exposing the third chromosome of *Burkholderia cepacia* complex strains  
642 as a virulence plasmid. *Mol Microbiol* 83:362–378.
- 643 30. Morrow JD, Cooper VS. 2012. Evolutionary effects of translocations in bacterial genomes.  
644 *Genome Biol Evol* 4:1256–1262.
- 645 31. Egan ES, Waldor MK. 2003. Distinct replication requirements for the two *Vibrio cholerae*  
646 chromosomes. *Cell* 114:521–530.
- 647 32. Rasmussen T, Jensen RB, Skovgaard O. 2007. The two chromosomes of *Vibrio cholerae*  
648 are initiated at different time points in the cell cycle. *Embo J* 26:3124–3131.
- 649 33. Duigou S, Knudsen KG, Skovgaard O, Egan ES, Lobner-Olesen A, Waldor MK. 2006.  
650 Independent control of replication initiation of the two *Vibrio cholerae* chromosomes by  
651 DnaA and RctB. *J Bacteriol* 188:6419–6424.
- 652 34. Baek JH, Chattoraj DK. 2014. Chromosome I controls chromosome II replication in *Vibrio*  
653 *cholerae*. *PLoS Genet* 10:e1004184.

- 654 35. Roesch A, Schmidbauer H. 2014. WaveletComp: Computational Wavelet Analysis. R  
655 package version 1.0. [https://CRAN.R-  
Proj.](https://CRAN.R-project.org/package=WaveletComp)
- 656 36. Cazelles B, Chavez M, Berteaux D, Menard F, Vik JO, Jenouvrier S, Stenseth NC. 2008.  
657 Wavelet analysis of ecological time series. *Oecologia* 156:287–304.
- 658 37. Donley N, Thayer MJ. 2013. DNA replication timing, genome stability and cancer late  
659 and/or delayed DNA replication timing is associated with increased genomic instability.  
660 *Semin Cancer Biol* 23:80–89.
- 661 38. Schuster-Böckler B, Lehner B. 2012. Chromatin organization is a major influence on  
662 regional mutation rates in human cancer cells. *Nature*.
- 663 39. Lawrence MS, Stojanov P, Polak P, Kryukov G V, Cibulskis K, Sivachenko A, Carter SL,  
664 Stewart C, Mermel CH, Roberts S a, Kiezun A, Hammerman PS, McKenna A, Drier Y, Zou  
665 L, Ramos AH, Pugh TJ, Stransky N, Helman E, Kim J, Sougnez C, Ambrogio L, Nickerson  
666 E, Shefler E, Cortés ML, Auclair D, Saksena G, Voet D, Noble M, DiCara D, Lin P,  
667 Lichtenstein L, Heiman DI, Fennell T, Imielinski M, Hernandez B, Hodis E, Baca S, Dulak  
668 AM, Lohr J, Landau D-A, Wu CJ, Melendez-Zajgla J, Hidalgo-Miranda A, Koren A,  
669 McCarroll S a, Mora J, Lee RS, Crompton B, Onofrio R, Parkin M, Winckler W, Ardlie K,  
670 Gabriel SB, Roberts CWM, Biegel J a, Stegmaier K, Bass AJ, Garraway L a, Meyerson M,  
671 Golub TR, Gordenin D a, Sunyaev S, Lander ES, Getz G. 2013. Mutational heterogeneity  
672 in cancer and the search for new cancer-associated genes. *Nature* 499:214–8.
- 673 40. Liu L, De S, Michor F. 2013. DNA replication timing and higher-order nuclear organization  
674 determine single-nucleotide substitution patterns in cancer genomes. *Nat Commun* 4:1–9.

- 675 41. Eisen J a, Heidelberg JF, White O, Salzberg SL. 2000. Evidence for symmetric  
676 chromosomal inversions around the replication origin in bacteria. *Genome Biol*  
677 1:research0011.1-0011.9.
- 678 42. Dettman JR, Rodrigue N, Kassen R. 2014. Genome-wide patterns of recombination in the  
679 opportunistic human pathogen *Pseudomonas aeruginosa*. *Genome Biol Evol* 7:18–34.
- 680 43. Baer CF, Miyamoto MM, Denver DR. 2007. Mutation rate variation in multicellular  
681 eukaryotes: causes and consequences. *Nat Rev Genet* 8:619–631.
- 682 44. Foster PL, Lee H, Popodi E, Townes JP, Tang H. 2015. Determinants of spontaneous  
683 mutation in the bacterium *Escherichia coli* as revealed by whole-genome sequencing. *Proc*  
684 *Natl Acad Sci* 112:E5990–E5999.
- 685 45. Schmidt KH, Reimers JM, Wright BE. 2006. The effect of promoter strength, supercoiling  
686 and secondary structure on mutation rates in *Escherichia coli*. *Mol Microbiol* 60:1251–  
687 1261.
- 688 46. Paul S, Million-Weaver S, Chattopadhyay S, Sokurenko E, Merrikk H. 2013. Accelerated  
689 gene evolution through replication-transcription conflicts. *Nature* 495:512–515.
- 690 47. Allen TE, Price ND, Joyce AR, Palsson B. 2006. Long-range periodic patterns in microbial  
691 genomes indicate significant multi-scale chromosomal organization. *PLoS Comput Biol*  
692 2:e2.
- 693 48. Fuchs RP, Fujii S. 2013. Translesion DNA synthesis and mutagenesis in prokaryotes. *Cold*  
694 *Spring Harb Perspect Biol* 5:1–22.
- 695 49. Cadet J, Douki T, Ravanat J-L. 2008. Oxidatively generated damage to the guanine moiety  
696 of DNA: mechanistic aspects and formation in cells. *Acc Chem Res* 41:1075–1083.

- 697 50. Long H, Miller SF, Strauss C, Zhao C, Cheng L, Ye Z, Griffin K, Te R, Lee H, Chen C-C,  
698 Lynch M. 2016. Antibiotic treatment enhances the genome-wide mutation rate of target  
699 cells. *Proc Natl Acad Sci* 113:E2498–E2505.
- 700 51. Sun L, Fuchs JA. 1992. *Escherichia coli* ribonucleotide reductase expression is cell cycle  
701 regulated. *Mol Biol Cell* 3:1095–1105.
- 702 52. Gon S, Camara JE, Klungsoyr HK, Crooke E, Skarstad K, Beckwith J. 2006. A novel  
703 regulatory mechanism couples deoxyribonucleotide synthesis and DNA replication in  
704 *Escherichia coli*. *EMBO J* 25:1137–1147.
- 705 53. Schaaper RM, Mathews CK. 2013. Mutational consequences of dNTP pool imbalances in  
706 *E. coli*. *DNA Repair* 12:73–79.
- 707 54. Ahluwalia D, Schaaper RM. 2013. Hypermutability and error catastrophe due to defects in  
708 ribonucleotide reductase. *Proc Natl Acad Sci* 110:18596–18601.
- 709 55. Stokke C, Waldminghaus T, Skarstad K. 2011. Replication patterns and organization of  
710 replication forks in *Vibrio cholerae*. *Microbiology* 157:695–708.
- 711 56. Mathews CK. 2015. Deoxyribonucleotide metabolism, mutagenesis and cancer. *Nat Rev*  
712 *Cancer* 15:528–539.
- 713 57. Poli J, Tsaponina O, Crabbé L, Keszthelyi A, Pantesco V, Chabes A, Lengronne A, Pasero  
714 P. 2012. dNTP pools determine fork progression and origin usage under replication stress.  
715 *EMBO J* 31:883–894.
- 716 58. Watt DL, Buckland RJ, Lujan SA, Kunkel TA, Chabes A. 2016. Genome-wide analysis of  
717 the specificity and mechanisms of replication infidelity driven by imbalanced dNTP pools.  
718 *Nucleic Acids Res* 44:1669–1680.

- 719 59. Schroeder JW, Randall JR, Hirst WG, O'Donnell ME, Simmons LA. 2017. Mutagenic cost  
720 of ribonucleotides in bacterial DNA. *Proc Natl Acad Sci* 114:11733–11738.
- 721 60. Schroeder JW, Yeesin P, Simmons LA, Wang JD. 2018. Sources of spontaneous  
722 mutagenesis in bacteria. *Crit Rev Biochem Mol Biol* 53:29–48.
- 723 61. Dillon MM, Sung W, Lynch M, S. C V. 2017. Genome-wide biases in the rate and  
724 molecular spectrum of spontaneous mutations in *Vibrio cholerae* and *Vibrio fischeri*. *Mol*  
725 *Biol Evol* 34:93–109.
- 726 62. Lynch M. 2007. The origins of genome architecture. Sinauer Associates, Sunderland (MA).
- 727 63. Strauss C, Long H, Patterson CE, Te R, Lynch M. 2017. Genome-wide mutation rate  
728 response to pH change in the coral reef. *mBio* 8:e01021-17.
- 729 64. Lässig M, Mustonen V, Walczak AM. 2017. Predicting evolution. *Nat Ecol Evol* 1:0077.
- 730 65. Val ME, Skovgaard O, Ducos-Galand M, Bland MJ, Mazel D. 2012. Genome engineering  
731 in *Vibrio cholerae*: A feasible approach to address biological issues. *Plos Genet*  
732 8:e1002472.
- 733 66. Heckman KL, Pease LR. 2007. Gene splicing and mutagenesis by PCR-driven overlap  
734 extension. *Nat Protoc* 2:924–932.
- 735 67. Datsenko KA, Wanner BL. 2000. One-step inactivation of chromosomal genes in  
736 *Escherichia coli* K-12 using PCR products. *Proc Natl Acad Sci U S A* 97:6640–6645.
- 737 68. Stabb E V., Ruby EG. 2002. RP4-based plasmids for conjugation between *Escherichia coli*  
738 and members of the *Vibrionaceae*. *Methods Enzymol* 358:413–426.

- 739 69. Ruby EG, Urbanowski M, Campbell J, Dunn A, Faini M, Gunsalus R, Lostroh P, Lupp C,  
740 McCann J, Millikan D, Schaefer A, Stabb E, Stevens A, Visick K, Whistler C, Greenberg  
741 EP. 2005. Complete genome sequence of *Vibrio fischeri*: A symbiotic bacterium with  
742 pathogenic congeners. *Proc Natl Acad Sci U S A* 102:3004–3009.
- 743 70. LiPuma JJ, Spilker T, Coenye T, Gonzalez CF. 2002. An epidemic *Burkholderia cepacia*  
744 complex strain identified in soil. *Lancet* 359:2002–2003.
- 745 71. Beaulaurier J, Zhang X, Zhu S, Sebra R, Rosenbluh C, Deikus G, Shen N, Munera D,  
746 Waldor MK, Chess A, Blaser MJ, Schadt EE, Fang G. 2015. Single molecule-level  
747 detection and long read-based phasing of epigenetic variations in bacterial methylomes.  
748 *Nat Commun* 6:7438.
- 749 72. Gao F, Zhang C-T. 2008. Ori-Finder: a web-based system for finding *oriC*s in unannotated  
750 bacterial genomes. *BMC Bioinformatics* 9:79–85.
- 751 73. Gao F, Luo H, Zhang CT. 2013. DoriC 5.0: an updated database of *oriC* regions in both  
752 bacterial and archaeal genomes. *Nucleic Acids Res* 41:D90–D93.
- 753

754 **FIGURE LEGENDS**

755

756 **Figure 1.** Patterns of base-substitution mutation (bpsm) rates at various size intervals  
757 extending clockwise from the origin of replication (*oriC*) in MMR-deficient mutation  
758 accumulation lineages of *V. fischeri* (A) and *V. cholerae* (B) on chromosome 1. Bpsm  
759 rates are calculated as the number of mutations observed within each interval, divided  
760 by the product of the total number of sites analyzed within that interval across all lines  
761 and the number of generations of mutation accumulation. The two intervals that meet at  
762 the terminus of replication (dotted red line) on each replicore are shorter than the  
763 interval length for that analysis, because the size of chromosome 1 is never exactly  
764 divisible by the interval length.

765

766 **Figure 2.** Relationship between base-substitution mutation (bpsm) rates in 100 Kb  
767 intervals on the right replicore with concurrently replicated 100 Kb intervals on the left  
768 replicore in MMR-deficient *Vibrio fischeri* (A) and *Vibrio cholerae* (B). Both linear  
769 regressions are significant on chr1 (*V. fischeri*:  $F = 10.98$ ,  $df = 13$ ,  $p = 0.0060$ ,  $r^2 = 0.46$ ;  
770 *V. cholerae*:  $F = 6.76$ ,  $df = 13$ ,  $p = 0.0221$ ,  $r^2 = 0.34$ ) but not on chr2 (*V. fischeri*:  $F =$   
771  $0.02$ ,  $df = 6$ ,  $p = 0.8910$ ,  $r^2 = 0.03 \times 10^{-1}$ ; *V. cholerae*:  $F = 0.06$ ,  $df = 4$ ,  $p = 0.8140$ ,  $r^2 =$   
772  $0.02$ ).

773

774 **Figure 3.** Patterns of base-substitution mutation (bpsm) rates in 100 Kb intervals  
775 extending clockwise from the origin of replication (*oriCI*) on chromosome 1 (chr1) and  
776 patterns of bpsm of concurrently replicated 100 Kb intervals on chromosome 2 (chr2) for

777 MMR-deficient *Vibrio fischeri* (A) and *Vibrio cholerae* (B). Patterns of bpsm rates on  
778 chr2 appear to map to those of concurrently replicated regions on chr1 in both species,  
779 but the linear regressions between concurrently replicated intervals are not significant  
780 on chr1 and chr2 in either *V. fischeri* or *V. cholerae* (*V. fischeri*:  $F = 0.62$ ,  $df = 14$ ,  $p =$   
781  $0.4442$ ,  $r^2 = 0.04$ ; *V. cholerae*:  $F = 0.07$ ,  $df = 10$ ,  $p = 0.7941$ ,  $r^2 = 0.01$ ).

782  
783 **Figure 4.** Wavelet power spectrum and resultant reconstruction of the patterns of base-  
784 substitution mutation (bpsm) rates in 100 Kb intervals extending clockwise from the  
785 *oriCI* region of chromosome 1 (A, B: *V. fischeri*; E, F: *V. cholerae*) and the *oriCII* region  
786 of chromosome 2 (C,D: *V. fischeri*; G,H: *V. cholerae*) using the MMR-deficient mutation  
787 accumulation lineages. Wavelet power analyses follow an interval color key (A, C, E,  
788 G), where colors code for the power values at each interval in the genome for all  
789 possible wave periods, from dark blue (low power) to dark red (high power). White  
790 contour lines denote significance cutoff of 0.1. Reconstructed series were generated  
791 using only the wave periods whose average power was significant over the entire  
792 interval (B, D, F, H).

793  
794 **Figure 5.** Patterns of base-substitution mutation (bpsm) rates in 100 Kb intervals  
795 extending clockwise from the origin of replication (*oriC*) on chromosome 1 (chr1) and  
796 concurrently replicated intervals of chromosome 2 (chr2) for WT (MMR+) *Vibrio fischeri*  
797 (A), *Vibrio cholerae* (B), and *Burkholderia cenocepacia* (C). *B. cenocepacia* also has a  
798 third chromosome, which is not shown. These visual patterns are not statistically  
799 significant, perhaps owing to low sample size: (linear regression; *Vf*-wt:  $F = 0.16$ ,  $df =$

800 14,  $p = 0.7001$ ,  $r^2 = 0.01$ ;  $Vc$ -wt:  $F = 2.72$ ,  $df = 10$ ,  $p = 0.1300$ ,  $r^2 = 0.21$ ;  $Bc$ -wt:  $F = 0.32$ ,  
801  $df = 30$ ,  $p = 0.5760$ ,  $r^2 = 0.01$ )

802

803 **Figure 6.** Hypothesized model of the relationship between replication timing,  
804 ribonucleotide reductase (RNR) activity, and the resulting availability of dNTPs per  
805 active replication fork. The model is fit to the *V. cholerae* genome with two  
806 chromosomes (chr) of 3.0 Mb and 1.1 Mb. RNR activity follows a wave that rises after  
807 the firing of the origin of chr1 and then steadily declines until additional origins fire. The  
808 chr2 origin should fire after ~950Kb of replication on each replicore of chr1 to ensure  
809 termination synchrony between chromosomes, stimulating a second wave of RNR  
810 activity. The right axis, in units of dNTP/fork, uses arbitrary relative units to depict how  
811 RNR activity is expected to increase dNTP pools to a maximum level (2.0) that is diluted  
812 by the number of concurrent, active forks. A,B: Under slow growth RNR activity rises  
813 and then falls to the baseline required to maintain synthesis. C,D: Faster growth  
814 requires a second round of replication. Note: further rounds of overlapping replication  
815 do not significantly alter predicted dNTPs/fork, the hypothesized driver of mutation-rate  
816 variability.

817

818

## 819 TABLES

820 **Table 1.** Number of base-substitution mutations (bpsms) in each mutation accumulation  
821 experiment, and the associated average number of bpsms in intervals of variable sizes.

MA Lines	No. of bpsm	500 Kb		250 Kb		100 Kb		50 Kb		25 Kb		10 Kb	
		Avg.	SEM	Avg.	SEM	Avg.	SEM	Avg.	SEM	Avg.	SEM	Avg.	SEM
<i>Vf</i> -mut	4313	499.00	35.82	253.50	13.77	101.05	3.12	50.53	1.26	25.26	0.51	10.08	0.18
<i>Vc</i> -mut	1022	141.50	21.14	65.33	6.23	25.47	1.53	12.51	0.59	6.22	0.25	2.50	0.09

<i>Vf</i> -wt	219	22.25	3.28	12.25	1.39	4.95	0.40	2.48	0.20	1.24	0.09	0.50	0.03
<i>Vc</i> -wt	138	18.00	3.09	8.75	0.95	3.42	0.30	1.72	0.14	0.83	0.07	0.34	0.03
<i>Bc</i> -wt	245	15.90	1.43	7.58	0.57	3.27	0.22	1.62	0.11	0.81	0.05	0.32	0.02

822

## 823 SUPPLEMENTAL MATERIAL

824 **Figure S1.** Design of the interval analysis used in this study to enable direct  
825 comparisons of base-substitution mutation (bpsm) rates of concurrently replicated  
826 regions on chromosome 1 (chr1) and chromosome 2 (chr2). A) For all multi-  
827 chromosome species analyzed in this study, secondary chromosomes are split at their  
828 origin of replication (*oriCI*), and mapped directly to concurrently replicated intervals in  
829 late replicating regions of chr1. All intervals on both chromosomes are thus relative to  
830 the initiation of replication of *oriCI*, and the boundaries of the intervals are consistent  
831 with their replication timing. B) Patterns of bpsm rates on the single chromosome of  
832 *Escherichia coli* MG1655 rph+  $\Delta$ *mutL*, derived from (20), show a wave-like mirrored  
833 pattern of bpsm rates on the two opposing replichores. If replication timing governs this  
834 pattern, a hypothetical secondary chromosome would be expected to mirror patterns of  
835 bpsm rates of late replicated regions on the primary chromosome.

836

837 **Figure S2.** Patterns of base-substitution mutation (bpsm) rates at various size intervals  
838 extending clockwise from the origin of replication (*oriCI*), in MMR-deficient mutation  
839 accumulation lineages of *Vibrio fischeri* (A) and *Vibrio cholerae* (B) on chromosome 2.  
840 All interval breakpoints are plotted relative to the initiation of replication of *oriCI* so that  
841 the boundaries of the intervals are at identical locations.

842

843 **Figure S3.** Cross-wavelet power spectrum plots comparing the patterns of base-  
844 substitution mutation (bpsm) rates in 100 Kb intervals extending clockwise from the  
845 *oriCI* region to those extending counterclockwise from the *oriCI* region in MMR-deficient

846 mutation accumulation lineages of *Vibrio fischeri* (A) and *Vibrio cholerae* (B). Plots were  
847 generated using the WaveletComp package for Computational Wavelet Analysis in R,  
848 using an interval color key, 100 simulations, and significant synchronicity cutoffs of  $p <$   
849  $0.1$  for contour (white lines) and  $p < 0.05$  for arrows. Colors represent the cross-wavelet  
850 power values at each interval in the genome for all possible wave periods, from dark  
851 blue (low power) to dark red (high power).

852  
853 **Figure S4:** Relationship between base-substitution mutation (bpsm) rates in 100 Kb  
854 intervals on the right replicore with concurrently replicated 100 Kb intervals on the left  
855 replicore for A:T>G:C (A) and G:C>A:T (B) bpsms in MMR-deficient *Vibrio fischeri* and  
856 C) A:T>G:C and D) G:C>A:T bpsms in MMR-deficient *Vibrio cholerae*. Only the  
857 relationship between G:C>A:T bpsm rates of concurrently replicated regions on chr1 is  
858 significantly positive (*Vf*: A:T>G:C: Chr1 -  $F = 1.77$ ,  $df = 13$ ,  $p = 0.2067$ ,  $r^2 = 0.12$ , Chr2 -  
859  $F = 3.26$ ,  $df = 6$ ,  $p = 0.1209$ ,  $r^2 = 0.35$ ; G:C>A:T: Chr1 -  $F = 13.32$ ,  $df = 13$ ,  $p = 0.0029$ ,  $r^2$   
860  $= 0.51$ , Chr2 -  $F = 0.17$ ,  $df = 6$ ,  $p = 0.6947$ ,  $r^2 = 0.03$ ; *Vc*: A:T>G:C: Chr1 -  $F = 0.24$ ,  $df =$   
861  $13$ ,  $p = 0.6313$ ,  $r^2 = 0.02$ , Chr2 -  $F = 1.74$ ,  $df = 4$ ,  $p = 0.2574$ ,  $r^2 = 0.30$ ; G:C>A:T: Chr1 -  
862  $F = 28.99$ ,  $df = 13$ ,  $p = 0.0001$ ,  $r^2 = 0.6904$ , Chr2 -  $F = 0.15$ ,  $df = 4$ ,  $p = 0.7209$ ,  $r^2 =$   
863  $0.04$ ).

864  
865 **Figure S5.** Effects of nucleotide context (trimer content) on bpsm rates. A) Heatmap of  
866 the context dependent base-substitution mutation (bpsm) rates for the 64 possible  
867 trimer combinations based on their lagging strand orientation in MMR-deficient mutation  
868 accumulation lineages of *Vibrio fischeri* (A) and *Vibrio cholerae* (B). B) Patterns of

869 base-substitution mutation (bpsm) rates in 100 Kb intervals extending clockwise from  
870 the origin of replication (*oriC*) in MMR-deficient mutation accumulation lineages of  
871 *Vibrio fischeri* (A) and *Vibrio cholerae* (B). Observed patterns of bpsm rates (gray lines)  
872 on chromosome 1 (Chr1) and chromosome 2 (Chr2) are compared to the expected  
873 patterns of bpsm rates (blue lines) based on the trimer content of the interval. Bpsm  
874 rates differ significantly from expectations based on trimer content: Chi-square test; *Vf*-  
875 mut: Chr1 -  $\chi^2 = 137.24$ , df = 29,  $p < 0.0001$ , Chr2 -  $\chi^2 = 20.04$ , df = 15,  $p = 0.1703$ ; *Vc*-  
876 mut: Chr1 -  $\chi^2 = 107.55$ , df = 29,  $p < 0.0001$ , Chr2 -  $\chi^2 = 14.87$ , df = 1,  $p = 0.1887$ )

877  
878 **Figure S6.** Relationship between base-substitution mutation rates (bpsm) with average  
879 synonymous substitution rates (left panels) and average non-synonymous substitution  
880 rates (right panels) of genes. *V. fischeri*, top panel, *V. cholerae*, bottom panel, Average  
881 synonymous and non-synonymous substitution rates were calculated using the average  
882 rates of all one-to-one orthologs shared between *V. fischeri* ES114 and *V. fischeri*  
883 MJ11, or between *V. cholerae* 2740-80 and *V. cholerae* HE-16 within each 100 Kb  
884 interval. Synonymous and non-synonymous substitution rates for individual genes were  
885 calculated as described in (Yang and Nielsen 2000). In *V. fischeri*, only the relationship  
886 between bpsm rates and synonymous substitution rates on chromosome 1 is significant  
887 (A: Chr1 -  $F = 8.32$ , df = 28,  $p = 0.0080$ ,  $r^2 = 0.23$ , Chr2 -  $F = 0.56$ , df = 14,  $p = 0.4681$ ,  
888  $r^2 = 0.04$ ; B: Chr1 -  $F = 2.14$ , df = 28,  $p = 0.1554$ ,  $r^2 = 0.07$ , Chr2 -  $F = 0.03$ , df = 14,  $p =$   
889  $0.8692$ ,  $r^2 = 0.02$ ), and in *V. cholerae*, none are significant (C: Chr1 -  $F = 0.43$ , df = 28,  
890  $p = 0.5186$ ,  $r^2 = 0.02$ , Chr2 -  $F = 0.49$ , df = 10,  $p = 0.5010$ ,  $r^2 = 0.05$ ; D: Chr1 -  $F = 0.02$ ,

891  $df = 28, p = 0.8897, r^2 = 0.01 \times 10^{-1}, \text{Chr2} - F = 0.01, df = 10, p = 0.9218, r^2 = 0.01 \times 10^{-1}$   
892  $^1$ ).

893

894

895 **Data Set S1.** Summary of all base-substitution mutations identified in each of the five  
896 mutation accumulation experiments carried out for this study, Chi-squared statistics of  
897 tests for uniform mutation rates, linear regression statistics for correlations between  
898 replicates and chromosomes, and residual fit of mutation rates to different  
899 chromosome intervals.

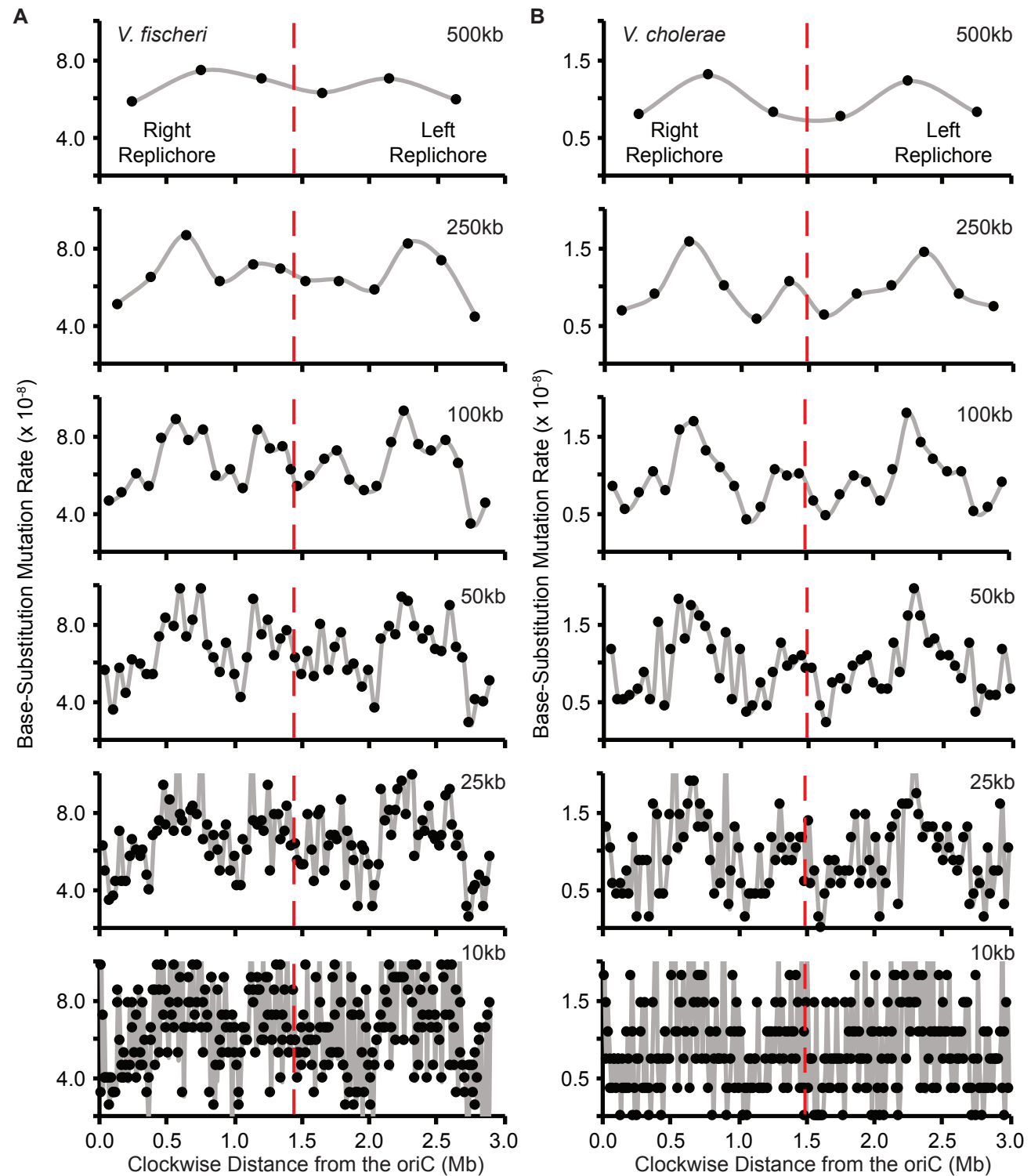


**Figure 1.** Patterns of base-substitution mutation (bpsm) rates at various size intervals extending clockwise from the origin of replication (*oriC*) in MMR-deficient mutation accumulation lineages of *V. fischeri* (A) and *V. cholerae* (B) on chromosome 1. Bpsm rates are calculated as the number of mutations observed within each interval, divided by the product of the total number of sites analyzed within that interval across all lines and the number of generations of mutation accumulation. The two intervals that meet at the terminus of replication (dotted red line) on each replichore are shorter than the interval length for that analysis, because the size of chromosome 1 is never exactly divisible by the interval length.

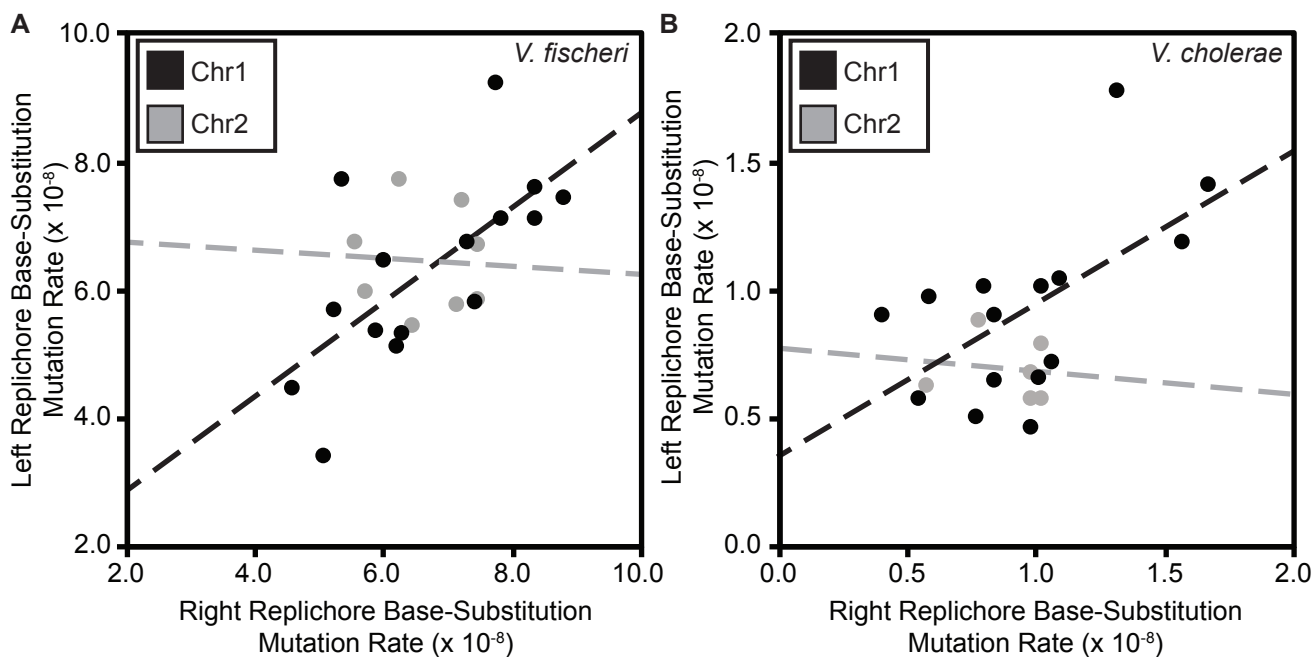


**Figure 2.** Relationship between base-substitution mutation (bpsm) rates in 100 Kb intervals on the right replicore with concurrently replicated 100 Kb intervals on the left replicore in MMR-deficient *Vibrio fischeri* (A) and *Vibrio cholerae* (B). Both linear regressions are significant on chr1 (*V. fischeri*:  $F = 10.98$ ,  $df = 13$ ,  $p = 0.0060$ ,  $r^2 = 0.46$ ; *V. cholerae*:  $F = 6.76$ ,  $df = 13$ ,  $p = 0.0221$ ,  $r^2 = 0.34$ ), but not on chr2 (*V. fischeri*:  $F = 0.02$ ,  $df = 6$ ,  $p = 0.8910$ ,  $r^2 = 0.03 \times 10^{-1}$ ; *V. cholerae*:  $F = 0.06$ ,  $df = 4$ ,  $p = 0.8140$ ,  $r^2 = 0.02$ ).

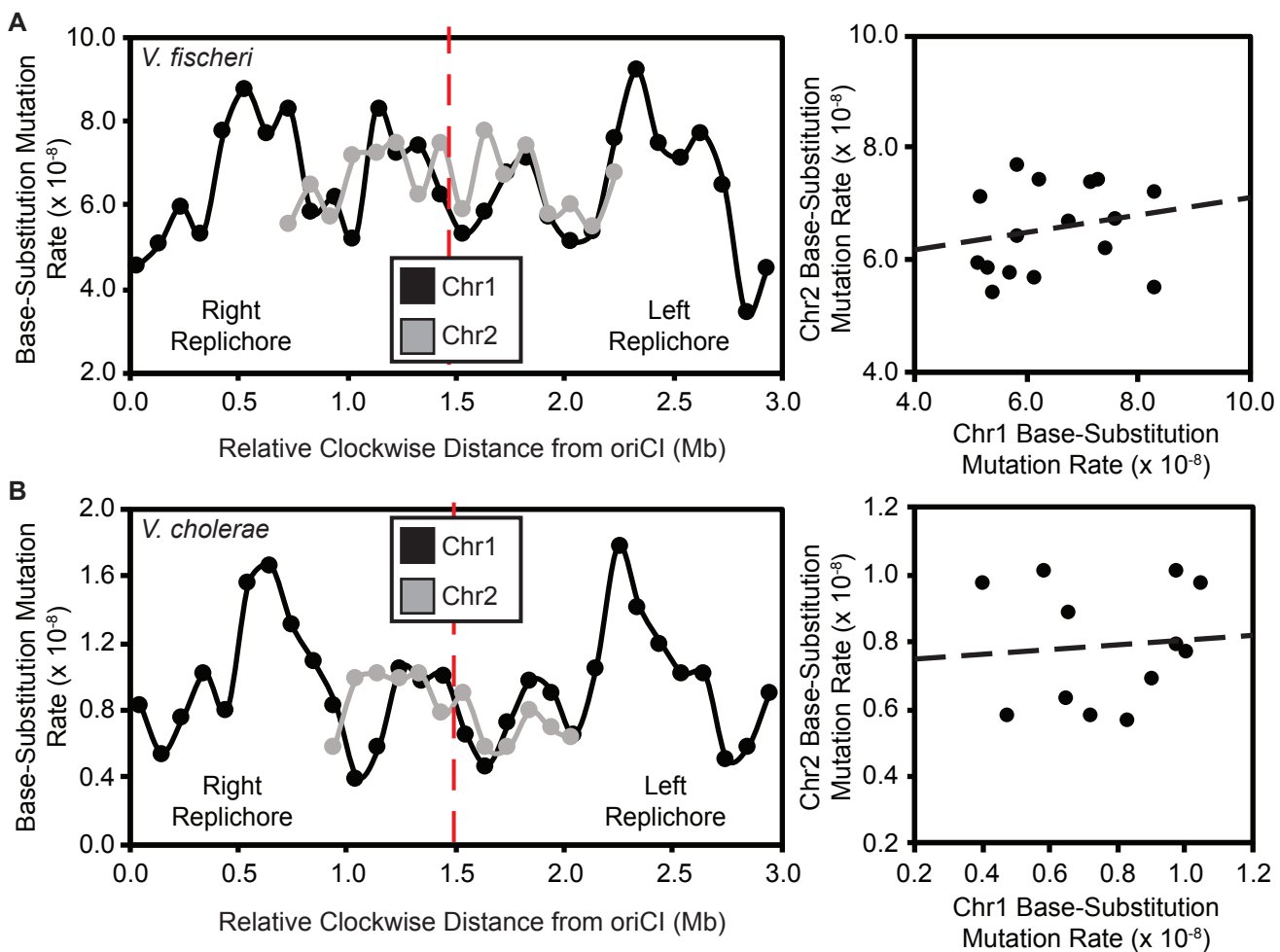


**Figure 3.** Patterns of base-substitution mutation (bpsm) rates in 100 Kb intervals extending clockwise from the origin of replication (*oriCI*) on chromosome 1 (chr1) and patterns of bpsm of concurrently replicated 100 Kb intervals on chromosome 2 (chr2) for MMR-deficient *Vibrio fischeri* (A) and *Vibrio cholerae* (B). Patterns of bpsm rates on chr2 appear to map to those of concurrently replicated regions on chr1 in both species, but the variance in bpsm rate between intervals is not sufficient to produce significant linear regressions between concurrently replicated intervals on chr1 and chr2 in either *V. fischeri* or *V. cholerae* (*V. fischeri*:  $F = 0.62$ ,  $df = 14$ ,  $p = 0.4442$ ,  $r^2 = 0.04$ ; *V. cholerae*:  $F = 0.07$ ,  $df = 10$ ,  $p = 0.7941$ ,  $r^2 = 0.01$ ).

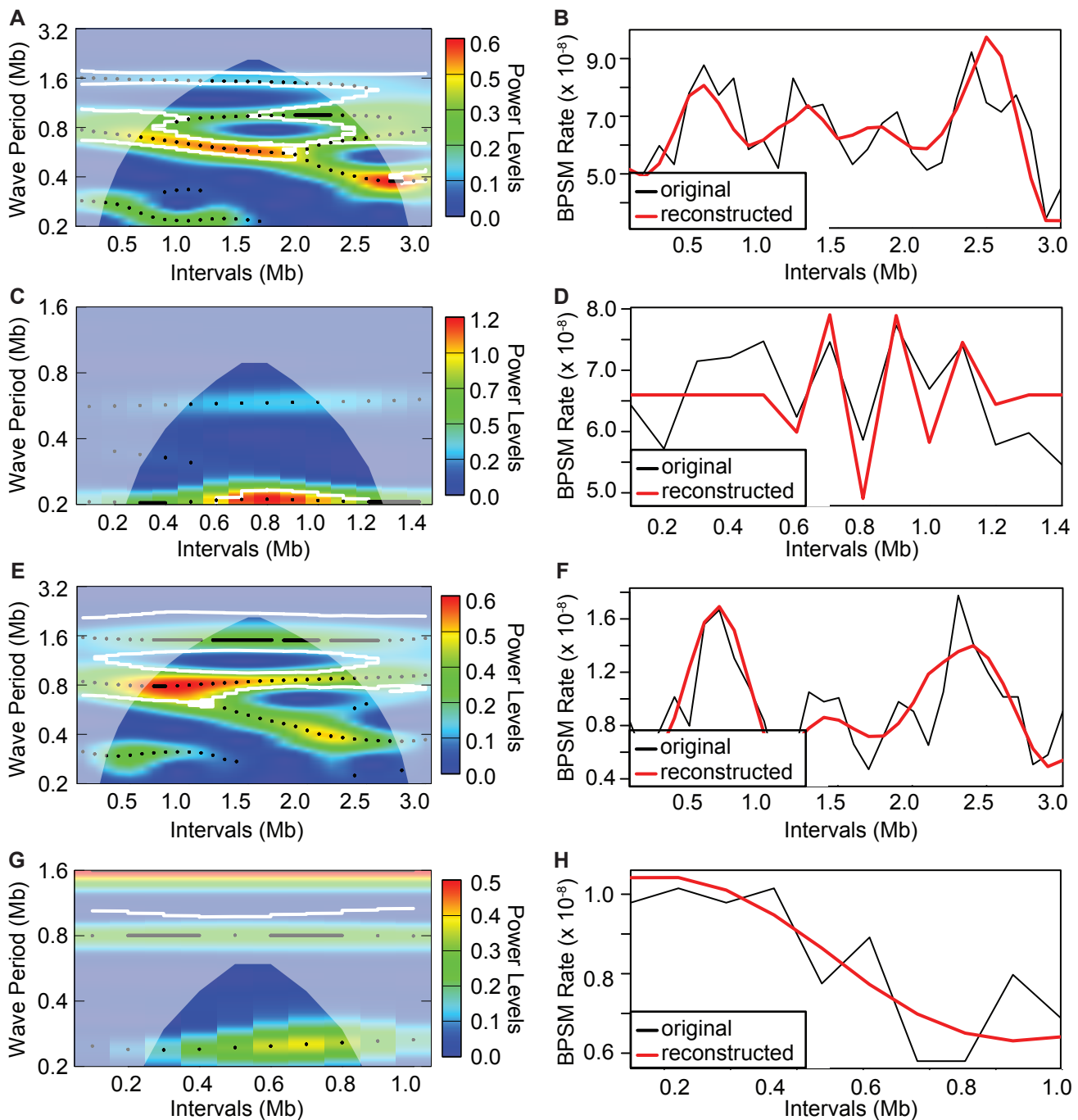


**Figure 4.** Wavelet power spectrum and resultant reconstruction of the patterns of base-substitution mutation (bpsm) rates in 100 Kb intervals extending clockwise from the *oriCI* region of chromosome 1 (A, B: *V. fischeri*; E, F: *V. cholerae*) and the *oriCII* region of chromosome 2 (C, D: *V. fischeri*; G, H: *V. cholerae*) using the MMR-deficient mutation accumulation lineages. White contour lines denote significance cutoff of 0.1 and wavelet power analyses follow an interval color key (A, C, E, G). Reconstructed series were generated using only the periods whose average power was significant over the entire interval (B, D, F, H).

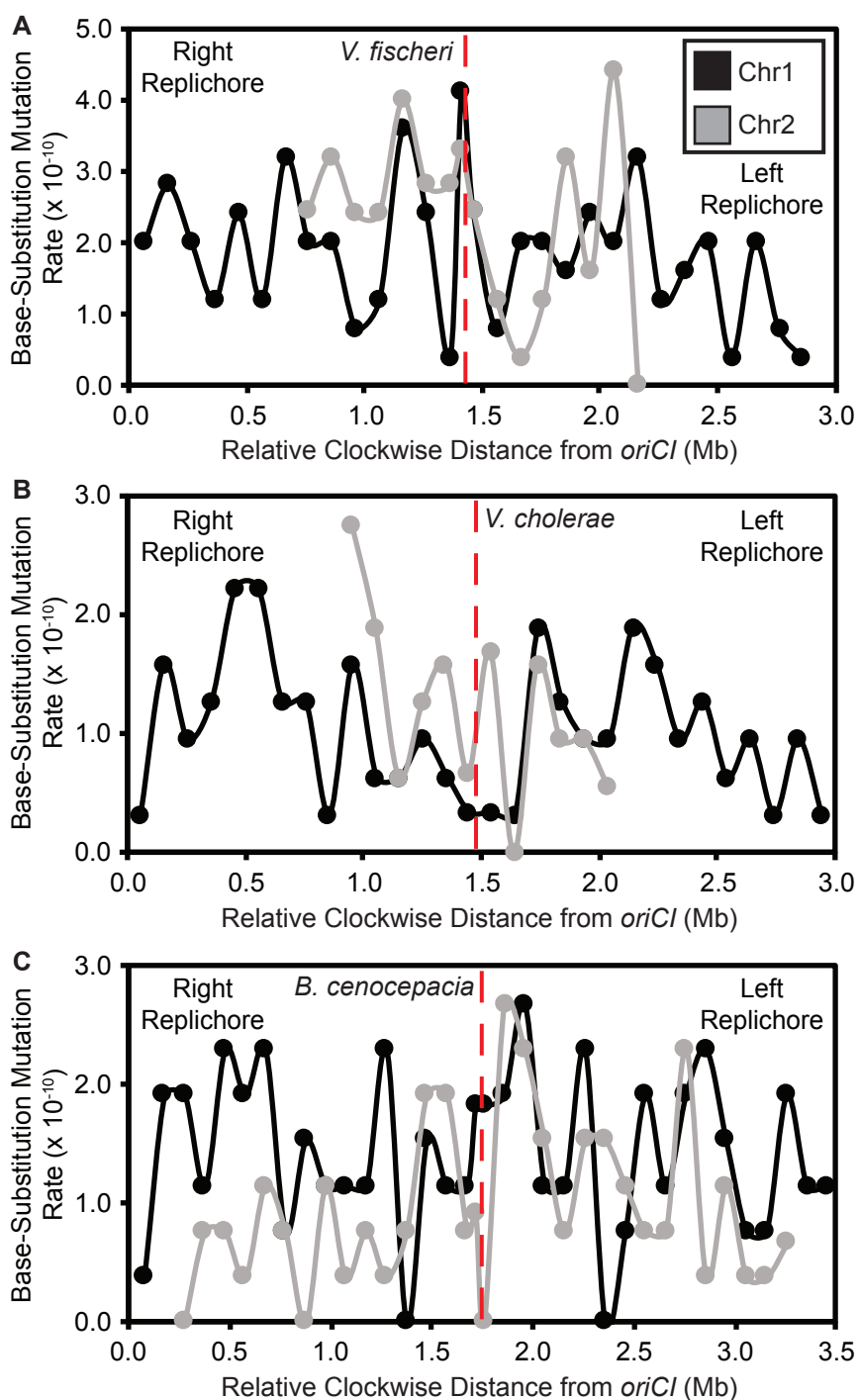


**Figure 5.** Patterns of base-substitution mutation (bpm) rates in 100 Kb intervals extending clockwise from the origin of replication (*oriC*) on chromosome 1 (chr1) and concurrently replicated intervals of chromosome 2 (chr2) for WT (MMR+) *Vibrio fischeri* (A), *Vibrio cholerae* (B), and *Burkholderia cenocepacia* (C). *B. cenocepacia* also has a third chromosome, which is not shown.

